Article

Soil Moisture Analysis by Means of Multispectral Images According to Land Use and Spatial Resolution on Andosols in the Colombian Andes

Maria Casamitjana [1,2,*] **, Maria C. Torres-Madroñero** [3] **, Jaime Bernal-Riobo** [1] **and Diego Varga** [2,*]

1   Corporación Colombiana de Investigación Agropecuaria—AGROSAVIA, Bogotá 250047, Colombia; jhbernal@agrosavia.co
2   Geography Department, University of Girona, Plaça Ferrater Mora, 1, 17004 Girona, Spain
3   Research Group on Smart Machine and Pattern Recognition, Instituto Tecnológico Metropolitano, Calle 54A No. 30 - 01, Barrio Boston, Medellin 050012, Colombia; mariatorres@itm.edu.co
*   Correspondence: mcasamitjana@agrosavia.co (M.C.); diego.varga@udg.edu (D.V.); Tel.: +34-972-418778 (D.V.)

Abstract: Surface soil moisture is an important hydrological parameter in agricultural areas. Periodic measurements in tropical mountain environments are poorly representative of larger areas, while satellite resolution is too coarse to be effective in these topographically varied landscapes, making spatial resolution an important parameter to consider. The Las Palmas catchment area near Medellin in Colombia is a vital water reservoir that stores considerable amounts of water in its andosol. In this tropical Andean setting, we use an unmanned aerial vehicle (UAV) with multispectral (visible, near infrared) sensors to determine the correlation of three agricultural land uses (potatoes, bare soil, and pasture) with surface soil moisture. Four vegetation indices (the perpendicular drought index, PDI; the normalized difference vegetation index, NDVI; the normalized difference water index, NDWI, and the soil-adjusted vegetation index, SAVI) were applied to UAV imagery and a 3 m resolution to estimate surface soil moisture through calibration with in situ field measurements. The results showed that on bare soil, the indices that best fit the soil moisture results are NDVI, NDWI and PDI on a detailed scale, whereas on potatoes crops, the NDWI is the index that correlates significantly with soil moisture, irrespective of the scale. Multispectral images and vegetation indices provide good soil moisture understanding in tropical mountain environments, with 3 m remote sensing images which are shown to be a good alternative to soil moisture analysis on pastures using the NDVI and UAV images for bare soil and potatoes.

Keywords: soil moisture; andosols; remote sensing

1. Introduction

In the area of agriculture, surface water content is known as soil moisture and is an important variable to consider and study to improve crops and yield. Depending on the soil moisture percentages, plant growth will be optimized, increasing nutrient absorption and the presence of microorganisms, regulating soil temperature, and affecting the speed of matter degradation and weathering processes. From a chemical point of view, soil moisture is essential for plants to undergo photosynthesis [1].

The Andes mountain range is a contrasting region with microclimates associated with its relief, where soil moisture is an important hydrological parameter that plays a vital role in the complex and vulnerable ecohydrology [2]. In agriculture, soil moisture is a complex parameter that can support soil sustainability [3]. In tropical countries such as Colombia, understanding soil moisture behavior

---

is important to control plant growth, particularly in drought periods. The existent inter-annual climate variability and consequent soil moisture changes can affect agricultural production and by extension planting dates, varieties, and other agricultural management practices [4]. The effect of land use on andosol water storage is poorly understood and implies a high variability of soil moisture surfaces. Wigmore et al. [5] recently stated that high-resolution remote sensing images are a good alternative to study large areas of land in the tropical Andes, providing unique insights into the surface and subsurface hydrologic processes that move and store water within these heterogeneous mountain environments.

One of the main challenges in agriculture and hydrology is estimating soil moisture content by means of remote sensing [6–8]. Remote sensing techniques can be categorized by the sensor—optical (visible and infrared), thermal, or microwave (active or passive)—and depending on the range of the electromagnetic spectrum monitor [9]. These sensors are placed in private and public satellites in space. For instance, SAR (synthetic aperture radar) sensors work by means of microwave pulses that are transmitted towards the Earth's surface by an antenna, measuring the microwave energy scattered back to the sensor, in addition to the time delay between the emission and the backscattered reception signal [10]. Remote optically sensed images are obtained by measuring the solar radiation reflected by targets on the ground. Radiation reflects, transmits, and absorbs differently at different wavelengths depending on the features of the materials on the Earth's surface. When the optical sensors have several channel detectors (3 to 15) sensitive to radiation within a narrow wavelength band, the result is a multispectral image based on multiple layers containing the brightness and spectral information of the observed Earth surface at each specific wavelength band. There are satellite initiatives that periodically capture multispectral images of the Earth's surface, including Landsat, Sentinel, Spot, and Ikonos [11]. While there have been several relevant initiatives to analyze soil moisture using satellite optical and radar sensors, which provide soil moisture products on several scales, the number of in situ soil moisture networks that are accessible and suited for satellite soil moisture evaluation is especially low for tropical regions [7].

Spatial soil moisture approximations are based on the indirect climate approach, with specific programs launched by ESA (European Space Agency) and NASA (National Aeronautics and Space Administration) in the USA. An important remote sensing project specific to the study of global soil moisture is the European Space Agency's Climate Change Initiative for Soil Moisture (ESA CCI SM), with a resolution of 25 km [12]. NASA launched its SMAP (Soil Moisture Active Passive) mission on January 2015, consisting of a radar and radiometer to monitor the amount of water in the top 5 cm of soils worldwide [6]. However, the radar failed in September of the same year, with the mission continuing to the present only with the radiometer data, which involve a resolution of 40 km.

There is an especially high variability of soil moisture in zones where land use, topography, and soil type are also highly variable [13]. Knowledge of soil moisture and its spatial distribution is of considerable importance to economic, social, hydrological, and agronomical planning. The scale required for each purpose varies, with initiatives at a resolution on a medium or global scale unsuitable for working on precision agriculture at a plot scale.

Over the last decade, the data obtained by unmanned aerial vehicles (UAV) have been intensively studied for agricultural applications given their flexibility of image acquisition and high spatial resolution, with customized cameras installed depending on the band (spectral resolution) and resolution requirements [14], especially including infrared bands used in several vegetation indices to monitor their states. Advances in UAV technology and sensor size, lower costs, global positioning systems (GPS), and pre-programmed flights have led to this knowledge gap being filled and a reduction in the spatial resolution of the most common current remote sensing systems. However, UAVs currently have several limitations related to weather conditions and re-visit times, in addition to being costly [15].

Soil mapping and image analysis are recent tools to simulate and monitor soil moisture [16]. The topographic wetness index (TWI) enables potential sites where moisture or water is accumulated to be identified by means of the geomorphologic analysis of the land using the DEM (digital elevation

model), considering that topography is a first-order control of the spatial variation of hydrological conditions [17]. The TWI is effective for studying soil moisture on a coarse scale with slope variability and is dependent on geology and the possible divergence between surface and subsurface conditions [17].

Multispectral satellite imagery is another approach to estimate soil moisture content [18] by means of the reflectance of the Earth's surface, although pixel spatial resolution is too coarse to be used on agriculture on a plot scale. Satellite measurements are also limited by their return period and are often impacted by cloud cover, particularly in tropical mountainous regions [5], reducing the available images to study the landscape. Soil reflectance is influenced by soil moisture and other intrinsic parameters, such as soil texture, mineral composition, and organic matter [19], affecting the absorption of different wavelengths. Recent laboratory studies have demonstrated the effect of soil moisture on reflectance for different orders of soils [20]. Organic matter and mineral composition affect short visible wavelengths and soil moisture in the NIR (near-infrared) and SWIR (shortwave infrared) spectral bands [19].

Regarding the spectral variations of water absorption, several multispectral indices using NIR and SWIR to analyze water content and soil moisture by means of optical sensors from space have been studied over the last decade [21–23]. For instance, the soil moisture of land covered by vegetation has been studied using indices such as the vegetation dryness index (VDI), the temperature vegetation dryness index (TVDI) [5], the enhanced vegetation index (EVI), the green coverage index (GCI) and, most commonly, the normalized difference vegetation index (NDVI), an enhanced vegetation index to determine vegetation status using drought as an indicator of soil moisture, and the normalized difference water index (NDWI), used to determine water bodies and areas where soil is saturated and additionally used to determine the vegetation hydric index, maximizing water reflectance. There are several methodologies to determine the NDWI. The Mc Feeters [24] equation uses the green band and the NIR band, optimizing vegetation moisture reflection and minimizing water bodies, whereas Dr Gao [25] determines the NDWI by means of the relationship between NIR and SWIR. Xu [26] later proposed the modified normalized difference water index (MNDWI), considering the green and SWIR bands. However, Chen et al. [27] state that soil moisture can cause side effects when using the SWIR band because its absorption is constrained to a reasonable extent. A soil-adjusted vegetation index such as the SAVI (soil-adjusted vegetation index) is used to reduce the soil effect, minimizing the related brightness by considering first-order soil vegetation interaction with soil-adjustment parameters [28]. Jeihouny et al. [29] use this index to map soil moisture by means of data mining, finding that SAVI is an important covariate in predicting soil moisture retention properties.

Another common methodology to estimate soil moisture by means of remote sensing is the trapezoid method, based on thermic and optical data regarding the Earth's surface [30]. This methodology has the problem that land surface temperature varies significantly with the ambient atmospheric parameters, while optical reflectance does not [31]. Starting from this assumption, some indices using optical observations have been proposed for soil moisture and drought monitoring based on triangular spaces from pixel distributions of optical observations in different electromagnetic frequency bands [31]. One of these triangular indices is the PDI (perpendicular drought index), designed by Ghulam et al. [32], which determines soil moisture for bare soils and low covers by means of the near infrared correlation of pixels. Amani and Parsian [22] evaluated the PDI, finding that it has some limitations that challenge its performance in areas with dense vegetation, but that it is highly effective for bare soils.

In this study, four indices (NDVI, NDWI, SAVI, and PDI) are evaluated to estimate soil moisture (SM) from high resolution images obtained by means of remote optical sensors and UAV flights in the highest part of the Las Palmas catchment area in Envigado, Colombia (See Figure 1). Soil moisture was evaluated according its land use on Andosol to determine an algorithm to correlate the studied indices with the soil moisture field data at different spatial resolutions. The four indices were evaluated to estimate soil moisture for three land uses (potatoes, bare soil and pasture). In addition, we analyze

these indices in several spatial resolution using re-sampled imagery from UAV. We demonstrate that the performance of these indices is conditioned to both land uses and spatial imagery resolution.
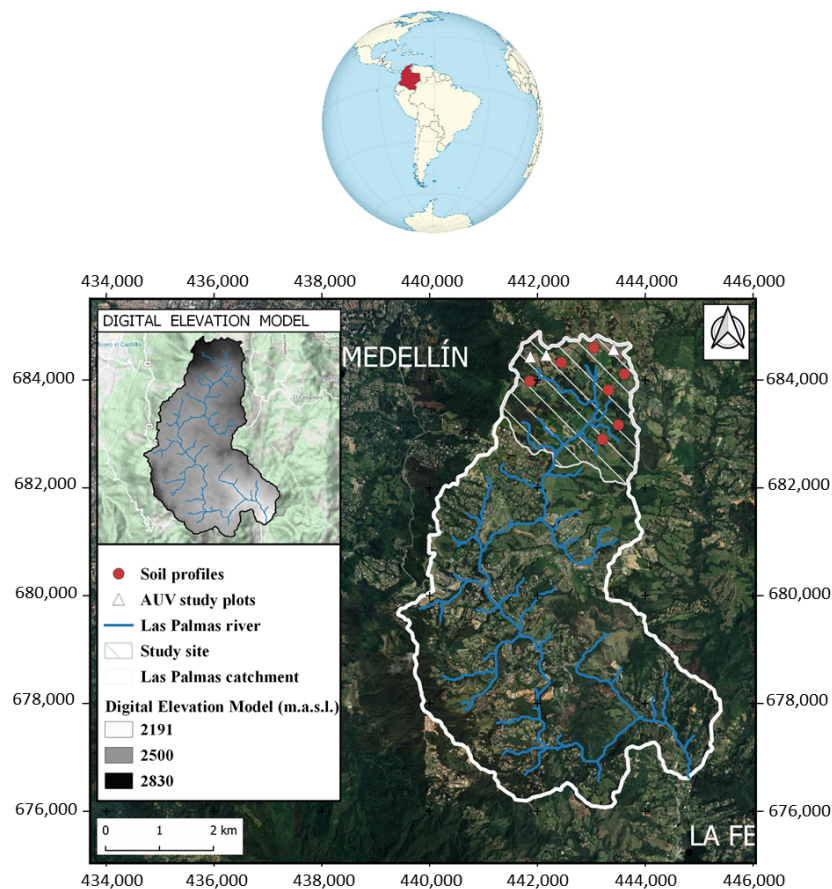
Figure 1. Study site location and unmanned aerial vehicle (UAV) flight sites by the digital elevation model (DEM 12.5 m) of the Las Palmas catchment area, Antioquia, Colombia, South America. Source: Current research.

2. Materials and Methods

2.1. Study Area

The study site is located in the Las Palmas catchment area in the central Andes mountain range. This catchment area supplies the water for La Fe reservoir, which guarantees the drinking water supply for the three million inhabitants of the Aburrá Valley metropolitan region [32]. This study site was selected to characterize soil moisture according to land use in an agricultural microcatchment area located in the upper section of Las Palmas catchment area in Envigado, Colombia (Figure 1).

There is an automated climatic EPM (Empresas Publicas Medellin) station in the upper part of the basin (44,3831, 68,4977 elevation: 2820 m.a.s.l.). The total annual precipitation average is 2500 mm/year (1980–2020), with a minimum annual precipitation in 1980 (1379.4 mm) and a maximum annual precipitation in 1999 (2837.2 mm). There are usually two dry seasons, from December to March and from June to August. The mean temperature for the same period was 18 °C (min 10.3 °C, max 22.3 °C).

The soil type in the study site is Andosol with its associated physical properties, making good water reservoirs with fluctuant hydrological properties [33]. Andosol is an unfertile soil due to its high degree of meteorization and the fact that it is derived from volcanic ashes that physically condition its porous system and structure, resulting in a high variation of soil moisture. Furthermore, the soil moisture regime in the study site is udic [34], meaning fewer than 90 cumulative days each year when

water is not available in the rooting zone in normal years. Perennial plants are adequately supplied with water most years. In most similar areas, two crops can be grown each year, but the available water is less reliable for some of the year and farmers often plant more drought-tolerant crops [35].

2.2. Procedure

The workflow used in this study is shown in Figure 2. It consisted of four steps: (a) preprocessing of datasets; (b) determination of vegetation indices; (c) analysis of the optimal resolutions; and (d) comparison of remote sensing variables for SM retrieval according to land use.
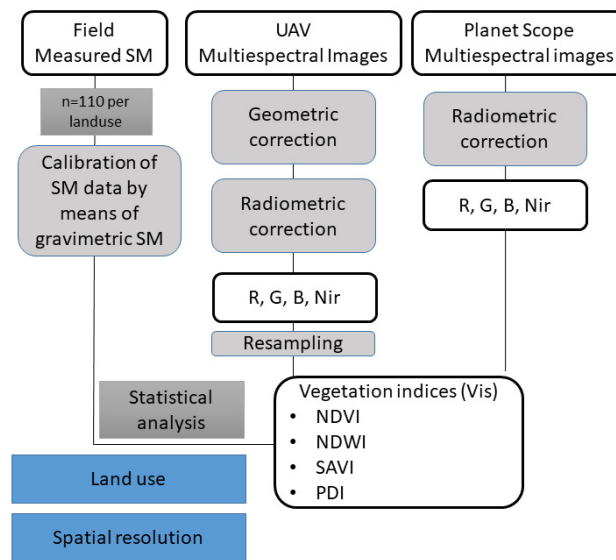
Figure 2. Workflow of the pursued methodology. R (Red), G (Green), B (Blue), NIR (Near Infra-Red). Source: Current research.

The field campaigns were carried out during the dry season on 5, 6, and 7 February 2019 to evaluate the soil moisture of three study plots measuring 1 ha per land use evaluated (i.e., pasture (*Pennisetum clandestinum*), potatoes (*Solanum tuberosum*), and bare soil) located in the highest part of the Las Palmas catchment area, Envigado, Colombia (Figure 1). Soil characterization of the study site was determined by means of 7 soil profile descriptions and pedologic and hydrological measurements (Figure 1, Table 1), analyzing NaF (sodium fluoride) reaction and pH, profile depth, volcanic ashes depth, infiltration, and field-saturated soil hydraulic conductivity (Kfs) in the upper soil layer. The reaction of sodium fluoride solution with soils and soil minerals is used as a parameter to determine the presence of amorphous minerals and hydromorphic soil conditions.

Table 1. Soil profile descriptions and associated hydrological and pedological variables. Kfs: field-saturated soil hydraulic conductivity.

Soil Profile	x	y	pH (0–10 cm)	Soil Texture (0–10 cm)	NaF Reaction	Depth A Profile	Depth Volcanic Ashes	K_{fs}	Infiltration T_{10}
1	841,661.7	1,174,433.7	5.1	Loam	Moderate	47	125	0.01574	39.3
2	841,812.6	1,174,370.8	5.2	Silty loam	Strong	34	106	0.01168	15
3	840,311.1	1,176,556.6	5.9	Loam	Strong	44	72	0.01815	7.33
4	840,298.9	1,176,382.1	5.5	Loam	Strong	44	150	0.00406	16.39
5	841,312.4	1,176,329.7	5.6	Loam	Strong	33	100	0.00899	134.33
6	841,552.3	1,176,249.2	5.3	Loam	Strong	26	120	0.015583	44.67
7	841,476.8	1,176,338.2	5	Loam	Strong	26	92	0.032536	123.33

The ground data used for the calibration and validation of the regression models were collected from 110 sampling points on each study plot, previously marked using 25 cm diameter polystyrene dishes and forming a regular grid with a distance of 10 m × 10 m between them (Figure 3). To verify the exact location of the sampling points, 5 sub-metric high-precision GPS spots were georeferred by means of a Topcon© Hiper V RTK, Livermore, CA, USA (Figure 3). On each studied plot, 110 sampling points were considered, and the soil moisture and temperature data were collected using a TDR sensor.

(a)   (b)   (c)
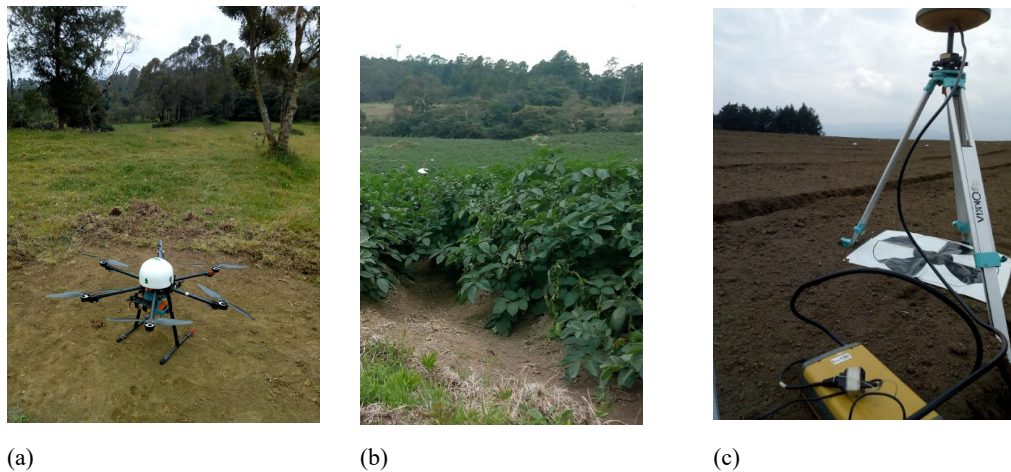
Figure 3. UAV flight over the study plots of pasture, potatoes, and bare soil. (**a**) UAV hexacopter on the pasture study plot, (**b**) potatoes study site, (**c**) Topcon submetric device on bare soil study site.

Simultaneously with the ground measurement, aerial images were acquired using a hexacopter UAV and a multispectral RedEdge camera, Micasense©, Seattle, WA, USA obtaining multiple sets of images in five spectral bands, blue (475 nm), green (560 nm), red (668 nm), red edge (717 nm) from the visible rank, and NIR (840 nm), to determine soil moisture reflectance (Figure 4). UgCS software, Riga, Latvia, Europe, was used for the automated drone mission planning. The images were later merged and postprocessed in the laboratory for geometric correction and calibration using the Pix4D© software, Prilly, Switzerland, Europe. Radiometric correction of the images PlanetScope©, San Francisco, CA, USA was carried out by means of the Qgis software, Gossau, Switzerland, Europe and the required parameters were obtained from the image metadata.
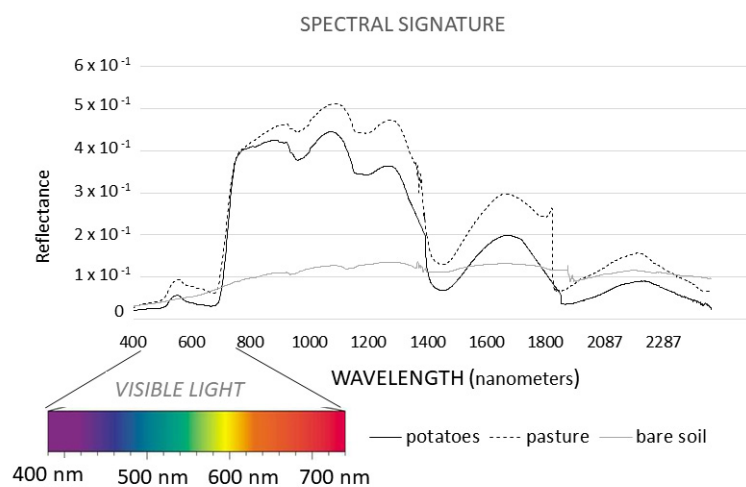
Figure 4. Reflectance according to the spectral region and wavelengths calculated on the study plots by means of a ASD FieldSpec 4 Hi-Res NG Spectroradiometer, Malvern Panalytical Ltd, Cambridge, UK (n = 50 per land use: potatoes, bare soil and pasture). Source: Current research.

The climatological information for the month prior to the sampling for the field experiment was collected at the EPM meteorological station located 450 m from the study plots, considering rainfall, temperature, and wind as influent parameters.

Optical Planet Scope 3m resolution images in four bands (R, G, B and NIR) were obtained for the same week as the ground measurements were taken. The images used were divided by bands and subsequently multiplied by the reflectance coefficient to convert the Digital number radiance, reescaled into an 8-bit digital number (DN) with a range between 0 and 255, into Top of Atmosphere (TOA) Reflectance.

The vegetation indices were computed using both the UAV and the planet scope images. According to the literature, the NDVI is defined as Equation (1), NDWI (Equation (2)), SAVI (Equation (3)) and PDI (perpendicular drought index) (Equation (4))

$$NDVI = (NIR - R)/(NIR + R) \tag{1}$$

$$NDWI = (GREEN - NIR)/(GREEN + NIR) \tag{2}$$

$$SAVI = [(NIR - R)/(NIR + R + L)] (1 + L) \tag{3}$$

$$PDI = 1/\sqrt{(M^2 + 1)}(R - (M \times NIR)) \tag{4}$$

To determine the PDI, a soil line was built by means of red and NIR reflectivity correlation of pixels on bare soil, where red was the independent variable and NIR the dependent variable [30]. This drought index was compiled using spatial characteristics of the soil moisture in red and NIR feature spaces to assess soil moisture stress. M is the slope of the soil line in the red–NIR spectral feature space, forming one edge of the triangle in the NIR–red spectral space represented by the soil line (Figure 5).

After extracting the pixel information from the spectral vegetation indices calculated from the UAV and satellite images, a regression analysis was carried out using the obtained field data.
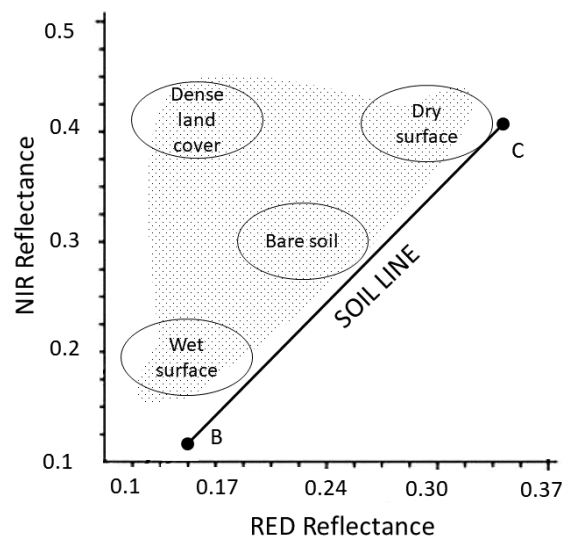
Figure 5. Near infrared versus red (NIR/R) correlation to obtain the soil line for the perpendicular drought index (PDI) calculation. Adapted from [32].

3. Results

3.1. Pedo-Hydrological Characterization of the Study Area

The study plots were located in areas with a udic soil moisture regime, a deep soil profile, 0–5% flat topography, and an isothermal temperature regime with well drained soils. The soils in the study

site have loam textures in the upper layers and a mean depth of volcanic ashes of 109.29 cm before saprolite presence. Table 1 shows the pedologic and hydrologic variables analyzed to determine the homogeneity of the study plots (located near to soil profiles 3 and 4 in the case of pasture and potatoes, and near to soil profiles 5, 6, and 7 in the case of the bare soil study plot).

3.2. The PDI According the Spatial Resolution

The NIR–red linear regression was obtained to calculate the soil line (Figure 5), and the M value was determined (Table 2) by means of Equation (4) to determine the PDI (perpendicular drought index).

Table 2. NIR–red linear equations to obtain the M value to calculate the PDI at 4 cm.

Land Use	NIR – Red Equation	M	PDI – SM (R^2)
Pastures	y = −0.4276x + 0.5824	−0.4276	0.4392
Potatoes	y = −3.9215x + 0.65	−3.9215	0.002
Bare soil	y = 0.5921x + 0.165	0.5921	0.5062

To validate the PDI, the in situ SM (soil moisture) data measurements every 10 m were compared with the PDI, obtaining the results shown in Figure 6 according to land use. Among these results, correlation is strongest between PDI and soil moisture under bare soil (R2 = 0.5062), followed by pasture and then potatoes.
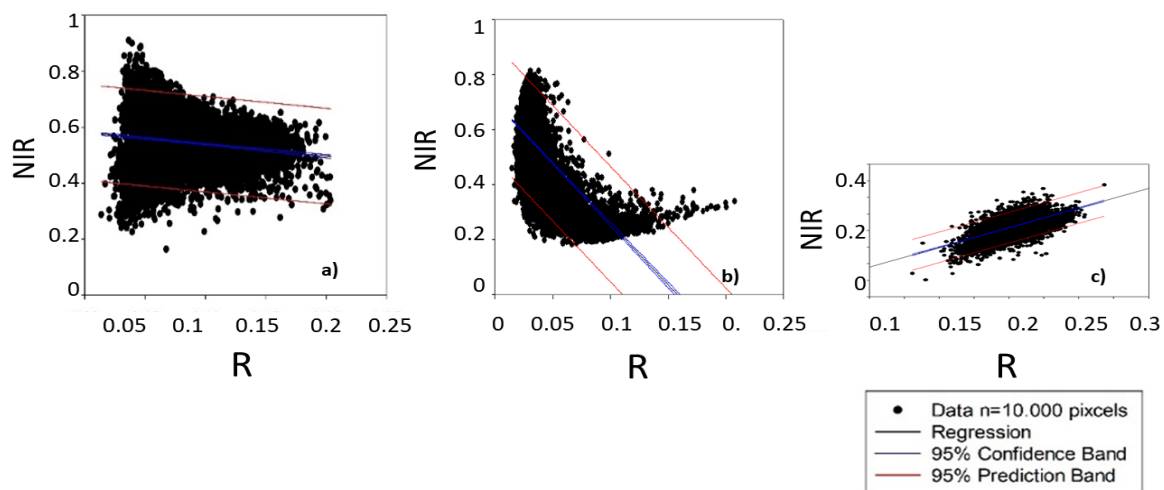
Figure 6. Polynomial linear correlations of NIR–R reflectance at 10,000 random points on the study site according to land use. (**a**) pasture study site, (**b**) potatoes study site, (**c**) bare soil study site. Source: Results of the current research.

Ghulam et al. [32] state that visible and near infrared spectral data are closely related to soil moisture at a soil depth of 10 cm.

The results obtained from repeating the same process at 3 m spatial resolution using the Planet Scope images are shown in Table 3. They show that there is a high correlation between the red and the NIR bands on satellite images with a spatial resolution of 300 cm, whereas the correlation between the PDI and soil moisture is lower than the UAV (unmanned aerial vehicle) 4 cm spatial resolution correlation.

A comparison of the PDI and soil moisture can be influenced by plant albedo and shade. The results shown in Figure 7 clearly demonstrate that potatoes at 4 cm resolution correlate less than bare soil and pastures at the same resolution.

Table 3. NIR– Red linear equations to obtain the M value to calculate the PDI at 300 cm spatial resolution.

Land Use	NIR – Red Equation (R^2)	M	PDI – SM (R^2)
Pastures	y = 0.9083x + 4.2942(R2 = 0.214)	0.9083	R2 = 0.141
Potatoes	y = −1.3897x + 6.562(R2 = 0.322)	−1.3897	R2 = 0.0191
Bare Soil	y = 1.6884x − 1.8164 (R2 = 0.465)	1.6884	R2 = 0.1137
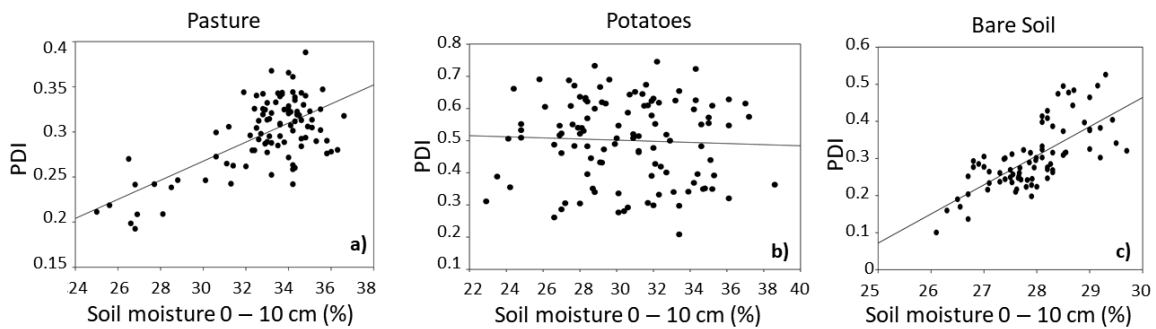
Figure 7. The PDI vs. soil moisture at 0–10 cm depth under different soil uses: (**a**) pasture R2 = 0.4392; (**b**) potatoes R2 = 0.002; (**c**) bare soil R2 = 0.5062) at UAV resolution (4 cm pixel).　n = 110. Source: Current research.

3.3. Soil Moisture vs. Vegetation Indices

For each land use, the SAVI, NDVI, and NDWI were determined from the UAV images (4 cm pixel), as can be seen in Figure 8.
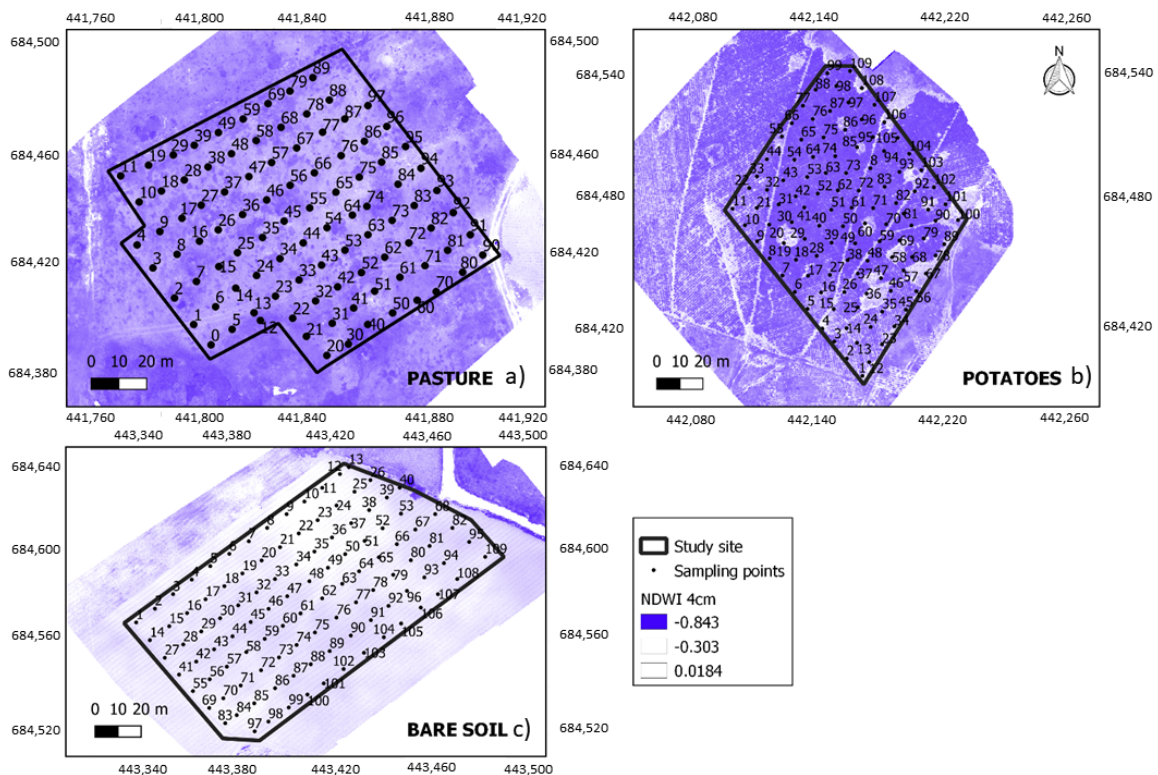
Figure 8. Normalized difference wetness index (NDWI) data obtained by means UAV composite images at 4 cm pixel resolution with the ground measurement location per land use. (**a**) pasture study site, (**b**) potatoes study site, (**c**) bare soil study site. Source: Current research.

Satellite Planet Analyst Scope images (300 cm pixel) were processed and then the same indices were determined per studied land use. Data for 12, 40, 100, 300 cm were obtained by means of an oversampling of the pixels of the UAV images on several scales, and from the means of the index values for each buffer zone of the sampling points. Posteriorly the georeferred data of each index were correlated with the ground soil moisture measurements.

The soil moisture data obtained from the sampling plots did not have a normal statistical distribution. The correlation between the measured soil moisture data and the indices obtained by means of the obtained images was analyzed by applying Spearman's rank correlation rho test according to the spatial resolution and land use. The following table shows these correlations (Table 4), where the triangle symbols denote the significant correlations.

It can be seen that there is an index that fits better, or presents a better correlation, with soil moisture for each of the land uses and resolutions studied.

Regarding pasture land use, soil moisture analysis by means of satellite images at 3 m resolution only had significant correlations with the NDVI. Pasture land use at a detailed 4 cm resolution scale showed a significant correlation between the PDI and soil moisture.

Under land use for potatoes, all the indices showed a positive correlation with soil moisture (Figure 9). Satellite images at 3 m resolution can be used to determine the soil moisture of potatoes land use using the NDWI and NDVI, that is, the indices that showed the best correlations (Table 4). At detailed resolution, only the NDWI showed a significant positive correlation with soil moisture (Figure 9).

The best representation to analyze soil moisture under bare soil is by means of the PDI with UAV images at high resolution, whereas the same index with a coarser satellite resolution (3 m) cannot be directly correlated with surface soil moisture (0 to 10 cm). At 3 m resolution, the NDVI and NDWI show the best significant correlations with soil moisture under bare soils, showing negative correlations (Figure 9).
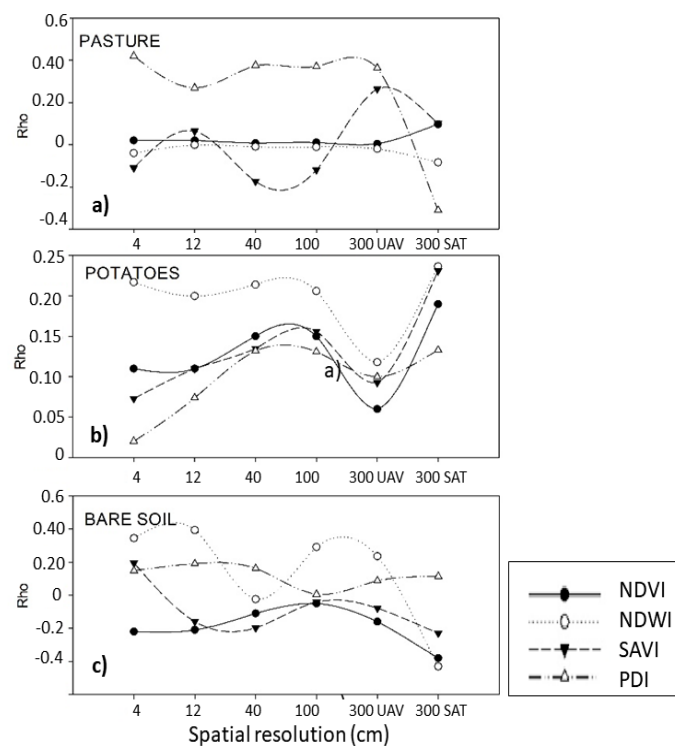
Figure 9. Rho correlation between the index and soil moisture according to land use and spatial resolution. (**a**) pasture study site, (**b**) potatoes study site, (**c**) bare soil study site. Source: Current research.

Table 4. Spearman's correlation coefficients (rho, *p*-value) for the normalized difference vegetation index (NDVI), the normalized difference water index (NDWI), the soil-adjusted vegetation index (SAVI), and the perpendicular drought index (PDI) regarding soil moisture at 0–10 cm depth under pasture, bare soil, and potatoes (n = 110).

Spatial Resolution	Pastures				Potatoes				Bare Soil			
	NDVI	NDWI	SAVI	PDI	NDVI	NDWI	SAVI	PDI	NDVI	NDWI	SAVI	PDI
4	0.02 (0.77)	−0.04 (0.67)	−0.11 (0.28)	0.42 (1.649×10^{-5})▲▲	0.11 (0.24)	0.21 (0.02)▲	0.07 (0.44)	0.002 (0.34)	−0.22 (0.03)▲	0.34 (0.0002)▲▲	0.19 (0.04)▲	0.14 (0.02)▲
12	0.02 (0.85)	−0.002 (0.97)	0.06 (0.55)	0.26 (0.007)▲▲	0.11 (0.28)	0.20 (0.03)▲	0.11 (0.23)	0.074 (0.47)	−0.21 (0.04)▲	0.39 (2.21×10^{-5})▲▲	−0.16 (0.09)	0.19 (0.04)▲
40	0.007 (0.94)	−0.01 (0.89)	−0.17 (0.10)	0.37 (0.0001)▲▲	0.15 (0.11)	0.21 (0.02)▲	0.13 (0.16)	0.13 (0.16)	−0.11 (0.25)	−0.02(0.79)	−0.19 (0.03)▲	0.16 (0.09)
100	0.01 (0.91)	−0.01 (0.90)	−0.12 (0.25)	0.37 (0.0001)▲▲	0.15 (0.11)	0.20 (0.03)▲	0.15 (0.10)	0.13 (0.17)	−0.05 (0.55)	0.29 (0.002)▲▲	−0.04 (0.64)	0.005 (0.09)
300	0.004 (0.96)	−0.02 (0.83)	0.26 (0.01)	0.36 (0.0002)▲▲	0.06 (0.51)	0.11 (0.02)▲	0.09 (0.33)	0.10 (0.29)	−0.16 (0.36)	0.23 (0.01)▲	−0.07 (0.41)	0.08 (0.36)
300sat	0.597 (0.0001)▲▲	−0.08 (0.40)	0.10 (0.39)	−0.31 (0.19)	0.19 (0.04)▲	0.23 (0.01)▲	0.23 (0.54)	0.13 (0.19)	−0.38 (5.6×10^{-5})▲▲	0.43 (9.16×10^{-6})▲▲	−0.23 (0.01)▲	0.11 (0.54)

Statistical significance: *p*-value is significant at 5% (▲) when it is lower than 0.05, and significant at 1% (▲▲) when it is lower than 0.01.

On bare soil land use, any resolution can be used to estimate soil moisture by means of optical images with the NDWI.

The index that performs the best on bare soil is the NDWI at any spatial resolution, the NDVI at 4 or 12 cm resolution or from satellite images, and the PDI at 4 cm resolution. On bare soil, the reflectance effect of the existent furrows every 2 m must be considered on coarser scales (Figure 3c), because the land roughness could cause differences on the averaged land reflectance.

4. Discussion

Farhan and Al Bakri [36] report that the NDVI mainly reflects seasonal vegetation conditions, showing higher correlations with seasonal soil moisture stress, whereas the PDI does not show this relationship.

The NDVI in this research was the vegetation index that performed better on coarser resolution than thinner spatial resolution, regardless of land use.

Both sensing drought indices, the NDVI and the PDI can explain soil moisture variability in all the studied land uses. One study [37] showed significant negative correlations in spring, summer, and autumn between the NDVI and soil moisture, whereas farmland showed a significant positive correlation between NDVI and soil moisture in winter. In the current research, NDVI positively correlates with potato and pasture land uses and negatively correlates with bare soil, possibly due to the higher evaporation on bare soils (Figure 9).

Bare soils are not affected by vegetation cover, so their reflectivity in red and NIR bands is only affected by the soil moisture content. If there is a decrease in soil moisture, the reflective+ity of the red and NIR bands increases [38]. When vegetation cover increases, reflectance in the NIR band is higher than in the red band. Where land use in the current study plot includes both soil and vegetation, the points scatter inside a triangular region in the NIR–R, as shown in Figure 5. These results on bare soils concur with laboratory reflectance studies [20].

Spatial resolution clearly determines the ability of a sensor to generate the indices that can successfully approximate soil moisture.

The NDVI produced no significant correlations with soil moisture on UAV images, whereas Planet Scope NDVI variants with their higher spectral and spatial resolution positively correlated with bare soils, concurring with [39]. The ease of calculating the NDVI and the high temporal resolution of the data may mean that Sentinel-2 Planet Scope may play a future role in early warning systems of drought, as it enables high-resolution vegetation condition monitoring, which may be useful in detecting the onset of agricultural drought.

In regard to the SAVI, this can only be used with a significant correlation to estimate the soil moisture of bare soils.

The NDWI was the index that performed best on detailed resolutions, especially to study the soil moisture of land use for vegetables such as potatoes, which is useful when considering precision agriculture.

Observing Table 4, it can be seen that on pasture, the most significant correlations are found on coarser scales, whereas bare soil and potatoes have better results on detailed resolutions. These results show that UAV with multispectral cameras are useful to evaluate bare soil and potato soil moisture at detailed scales, and, above all, with the NDWI, SAVI and PDI.

5. Conclusions

On bare soil, the indices that best fit with the soil moisture results were the NDVI, the NDWI, and the PDI on a detailed scale. In contrast, Amani et al. [21] found that bare soils have good significance on a coarse scale with Landsat8 images in arid environments. These results are in line with those of a recent sub-metric soil moisture study using UAV and multispectral images in tropical conditions in Peru [5].

Under potato crops, the NDWI correlates significantly with soil moisture irrespective of the scale of the analyzed image under potato land use.

The PDI is the index that correlates the highest with detailed scales, showing better results on pasture than on potatoes or bare soil. In regard to pastures at a coarser resolution, the NDVI showed the best correlation with soil moisture. These results are relevant due to the fact that the pasture is an extensive crop in Colombia and soil moisture monitoring can be useful to realize environmental studies of multitemporal changes of this important hydrological parameter.

A UAV soil moisture study [40] on Karst heterogeneous landscapes determined that the optimal resolution to analyze soil moisture by means of DEMs is 7 m, and that soil moisture variability is mainly explained by the vegetation type (35.7%), which concurs with the results of the current research.

The study of soil moisture with UAVs study presents several advantages over conventional platforms such as satellites, including the fact that they fly at lower altitudes, increasing the spatial resolution of the images, and cost less than private remote sensing images, allowing for more frequent monitoring. For average-size farms in Colombia, high-resolution remote sensing at 3 m such as Planet Scope combined with UAV data can be used to estimate soil moisture for the evaluated land uses. Remote sensing indices are currently being tested and improved to propose proxies that reflect the physiological status of crops under changing environmental conditions, and they can be used to determine plant water status for several crop species.

The best scale to study soil surface moisture with optical images is at 3m resolution, which can determine soil moisture at a depth of 0 to 10 cm using either the NDWI or NDVI according to its land use. None of the indices can be used for all crops or land uses with the same resolution. A prior classification of land use is needed to study soil moisture effectively due to the effect of vegetation on soil moisture at depths of 0 to 10cm, as supported by Ghulam et al. [32], who state that visible and near infrared spectral data have a close relationship with soil moisture at a soil depth of 10 cm.

According to land use as a means to determine soil moisture, a different index and resolution were found to provide the most accurate results; that is, resolutions of 3 m appropriate to study soil moisture under pasture, potatoes and bare soil using NDVI correlations with soil moisture in Andosols.

References

1.　Li, S.; Pezeshki, S.R.; Goodwin, S. Effects of soil moisture regimes on photosynthesis and growth in cattail (Typha latifolia). *Acta Oecologica* **2004**, *25*, 17–22. [CrossRef]

2.　Wright, C.; Kagawa-Viviani, A.; Gerlein-Safdi, C.; Mosquera, G.M.; Poca, M.; Tseng, H.; Chun, K.P. Advancing ecohydrology in the changing tropics: Perspectives from early career scientists. *Ecohydrology* **2018**, *11*, 112–125. [CrossRef]

3.　Firman Ghazali, M.; Wikantika, K.; Budi Harto, A.; Kondoh, A. Generating soil salinity, soil moisture, soil pH from satellite imagery and its analysis. *Inf. Process. Agric.* **2019**. [CrossRef]

4.　Esquivel, A.; Llanos-Herrera, L.; Agudelo, D.; Prager, S.D.; Fernandes, K.; Rojas, A.; Valencia, J.J.; Ramirez-Villegrasa, J. Predictability of seasonal precipitation across major crop growing areas in Colombia. *Clim. Serv.* **2018**, *12*, 36–47. [CrossRef]

5. Wigmore, O.; Marka, B.; McKenzie, J.; Baraerd, M.; Lautze, L. Sub-metre mapping of surface soil moisture in proglacial valleys of the tropical Andes using a multispectral unmanned aerial vehicle. *Remote. Sens. Environ.* **2019**, *222*, 104–118. [CrossRef]

6. Entekhabi, D.; Nioku, E.G.; O'Neill, P.E.; Kellogg, K.H.; Crow, W.T.; Edelstein, W.N.; Entin, J.K.; Goodman, S.D.; Jackson, T.J.; Johnson, J.; et al. The Soil Moisture Active Passive (SMAP) Mission. *Proc. IEEE* **2010**, *98*, 704–716. [CrossRef]

7. Gruber, A.; De Lannoy, G.; Albergel, C.; Al-Yaari, A.; Brocca, L.; Calvet, J.C.; Colliander, A.; Cosh, M.; Crow, W.; Dorigo, W.; et al. Validation practices for satellite soil moisture retrievals: What are (the) errors? *Remote Sens. Environ.* **2020**, *244*, 111806. [CrossRef]

8. Albergel, C.; de Rosnay, P.; Gruhier, C.; Muñoz-Sabater, J.; Hasenauer, S.; Isaksen, L.; Kerr, Y.; Wagner, W. Evaluation of remotely sensed and modelled soil moisture products using global ground-based in situ observations. *Remote Sens. Environ.* **2020**, *118*, 215–226. [CrossRef]

9. Wang, L.; Qu, J.J. Satellite remote sensing applications for surface soil moisture monitoring: A review. *Front. Earth Sci. China* **2009**, *3*, 237–247. [CrossRef]

10. Lievens, H.; Martens, B.; Verhoest, N.E.C.; Hahn, S.; Reichle, R.H.; Miralles, D.G. Assimilation of global radar backscatter and radiometer brightness temperature observations to improve soil moisture and land evaporation estimates. *Remote Sens. Environ.* **2017**, *18*, 194–210. [CrossRef]

11. He, Y.; Weng, Q. *High Spatial Resolution Remote Sensing. Data, Analysis and Applications 2018. Taylor & Francis Series in Imaging Science*; CRC Press: New York, NY, USA, 2018; ISBN 9781498761682.

12. Gruber, A.; Scanlon, T.; van der Schalie, R.; Wagner, W.; Dorigo, W. Evolution of the ESA CCI Soil Moisture climate data records and their underlying merging methodology. *Earth Syst. Sci. Data* **2019**, *11*, 717–739. [CrossRef]

13. Vicente-Serrano, S.; Begueria, S.; Lorenzo, J.; Camarero, J.; Lopez.Moreno, J.; Azorin-Molina, C.; Revuelto, J.; Moran-Tejeda, E.; Sanchez-Lorenzo, A. Performance of Drought Indices for Ecological, Agricultural, and Hydrological Applications. *Earth Interact.* **2012**, *16*, 1–27. [CrossRef]

14. Jelev, G.; Dimitrov, P.; Kamenova, I.; Ilieva, I.; Roumenina, E.; Filchev, L.; Gikov, A.; Banov, M.; Krasteva, V.; Kolchakov, V.; et al. Using UAV Spectral Vegetation Indices for Estimation and Mapping of Biophysical Variables in Winter Wheat. In *Digital Earth Observation, Proceedings of the 39th European Association of Remote Sensing Laboratories Symposium & 43rd General Assembly, Salzburg, Austria, 1–4 July 2019*; Riedler, B., Lettner, S., Lang, S., Tiede, D., Eds.; University of Salzburg: Salzburg, Austria, 2019.

15. Gago, J.; Douthe, C.; Coopman, R.E.; Gallego, P.P.; Ribas-Carbo, M.; Flexas, J.; Escalona, J.; Medrano, H. UAVs challenge to assess water stress for sustainable agriculture. *Agric. Water Manag.* **2015**, *153*, 9–19. [CrossRef]

16. Montoani Silva, B.; Godinho Silva, S.H.; de Oliveira, G.H.; Caspar Rosa Peters, P.H.; Reis dos Santos, W.J.; CuriI, N. Soil Moisture Assessed by Digital Mapping Techniques and Its Field Validation. *Ciênc. Agrotec.* **2014**, *38*, 140–148. [CrossRef]

17. Sørensen, R.; Zinko, U.; Seibert, J. On the calculation of the topographic wetness index: Evaluation of different methods based on field observations. *Hydrol. Earth Syst. Sci.* **2006**, *10*, 101–112. [CrossRef]

18. Shafian, S.; Maas, S. Index of Soil Moisture Using Raw Landsat Image Digital Count Data in Texas High Plains. *Remote Sens.* **2015**, *7*, 2352–2372. [CrossRef]

19. Wang, L.; Qu, J.J.; Hao, X.; Zhu, Q. Sensitivity studies of the moisture effects on MODIS SWIR reflectance and vegetation water indices. *Int. J. Remote Sens.* **2008**, *29*, 7065–7075. [CrossRef]

20. Fabre, S.; Briottet, X.; Lesaignoux, A. Estimation of Soil Moisture Content from the Spectral Reflectance of Bare Soils in the 0.4–2.5 μm Domain. *Sensors (Basel)* **2015**, *15*, 3262–3281. [CrossRef]

21. Lobell, D.B.; Asner, G.P. Moisture Effects On Soil Reflectance. *Soil Sci. Soc. Am. J.* **2002**, *66*, 722–727. [CrossRef]

22. Amani, M.; Parsian, S.; MirMazloumi, S.M.; Aieneh, O. Two new soil moisture indices based on the NIR-red triangle space of Landsat-8 data. *Int. J. Appl. Earth Obs. Geoinf.* **2016**, *50*, 176–186. [CrossRef]

23. Mohseni, F.; Mokhtarzade, M. A new soil moisture index driven from an adapted long-term, temperature-vegetation scatter plot using MODIS data. *J. Hydrol.* **2020**, *581*. [CrossRef]

24. McFeeter, S.K. The use of the Normalized Difference Water Index (NDWI) in the delineation of open water features. *Int. J. Remote Sens.* **1996**, *17*, 7. [CrossRef]

25. Gao, A. NDWI—A normalized difference water index for remote sensing of vegetation liquid water from space. *Remote Sens. Environ.* **1996**, *58*, 257–266. [CrossRef]

26. Xu, H. Modification of normalised difference water index (NDWI) to enhance open water features in remotely sensed imagery. *Int. J. Remote Sens.* **2006**, *27*, 3025–3033. [CrossRef]

27. Chen, X.; Guo, Z.; Chen, J.; Yang, W.; Yao, Y.; Zhang, C.; Cui, X.; Cao, X. Replacing the Red Band with the Red-SWIR Band (0.74ρred+0.26ρswir) Can Reduce the Sensitivity of Vegetation Indices to Soil Background. *Remote Sens.* **2019**, *11*, 851. [CrossRef]

28. Qi, J.; Chehbouni, A.; Huete, A.R.; Kerr, Y.H.; Sorooshian, S.A. Modified soil adjusted vegetation index. *Remote Sens. Environ.* **1994**, *48*, 119–126. [CrossRef]

29. Jeihounia, M.; Alavipanah, S.K.; Toomaniana, A.; Jafarzadeh, A.A. Digital mapping of soil moisture retention properties using solely satellite based data and data mining techniques. *J. Hydrol.* **2019**, *585*, 124786. [CrossRef]

30. Nemani, R.; Pierce, L.; Running, S.; Goward, S. Developing satellite-derived estimates of surface moisture status. *J. Appl. Meteorol.* **1993**, *32*, 548–557. [CrossRef]

31. Sadeghi, M.; Babaeian, E.; Tuller, M.; Jones, S.B. The optical trapezoid model: A novel approach to remote sensing of soil moisture applied to Sentinel-2 and Landsat-8 observations. *Remote Sens. Environ.* **2017**, *198*, 52–68. [CrossRef]

32. Ghulam, A.; Qin, Q.; Zhan, Z. Designing of the perpendicular drought index. *Environ. Geol.* **2007**, *52*, 1045–1052. [CrossRef]

33. Salazar, M.P. Water Distribution and Drainage Systems of Aburrá Valley, Colombia—Empresas Públicas de Medellín, E.S.P. *Procedia Eng.* **2017**, *186*, 1877–7058.

34. Casamitjana, M.; Loaiza, J.C. Propiedades físicas e hidrológicas en suelos derivados de cenizas volcánicas. In *Movimientos en Masa*; Casamitjana, Sidle, Eds.; Fondo Editorial EIA: Medellín, Colombia, 2019; ISBN 978-958-52367-0-7.

35. Abera, G.; Wolde-Meskel, A. Soil properties [35and soil organic carbon stocks of tropical andosol under different land uses. *Open J. Soil Sci.* **2013**, *3*, 153–162. [CrossRef]

36. Farhan, I.; Al-Bakri, J. Detection of a Real Time Remote Sensing Indices and Soil Moisture for Drought Monitoring and Assessment in Jordan. *Open J. Geol.* **2019**, *9*, 1048–1068. [CrossRef]

37. West, H.; Quinn, N.; Horswell, M.; White, P. Assessing Vegetation Response to Soil Moisture Fluctuation under Extreme Drought Using Sentinel-2. *Water* **2018**, *10*, 838. [CrossRef]

38. Zhang, J.; Zhang, Q.; Bao, A.; Wang, Y. A New Remote Sensing Dryness Index Based on the Near-Infrared and Red Spectral Space. *Remote Sens.* **2019**, *11*, 456. [CrossRef]

39. Chi, Y.; Sun, Y.; Sun, Y.; Liu, S.; Fu, Z. Multi-temporal characterization of land surface temperature and its relationships with normalized difference vegetation index and soil moisture content in the Yellow River Delta, China. *Glob. Ecol. Conserv.* **2020**, *23*, e01092. [CrossRef]

40. Luo, W.; Xianli, X.; Wen, X.; Wen, L.; Meixian, L.; Zhenwei, L.; Tao, P.; Chaohao, X.; Yaohuam, Z.; Ronfei, Z. UAV based soil moisture remote sensing in a karst mountainous catchment. *CATENA* **2019**, *174*, 478–489. [CrossRef]